Front. Struct. Civ. Eng. 2020, 14(1): 1–9
https://doi.org/10.1007/s11709-019-0541-7

RESEARCH ARTICLE

Fused structures for safer and more economical constructions

Yu-Fei WU[a], Ying-Wu ZHOU[b], Biao HU[b], Xiaoxu HUANG[b], Scott SMITH[c*]

[a] *School of Engineering, RMIT University, Melbourne, VIC 3001, Australia*
[b] *Guangdong Provincial Key Laboratory of Durability for Marine Civil Engineering, Shenzhen University, Shenzhen 518061, China*
[c] *School of Civil, Environmental and Mining Engineering, The University of Adelaide, South Australia 5005, Australia*
[*] *Corresponding author. E-mail: scott.smith@adelaide.au*

ABSTRACT Safety margin and construction costs are two conflicting goals for a structure. By providing a fuse in a structure that is triggered at a certain level of over-loading, further increase of loading is prohibited and failure of the structure is changed to a safer mode. As overloading is controlled and a safer failure mode is enforced, a fused structure requires a smaller safety factor thus leading to more economical construction without compromising safety. The use of a fuse will also facilitate safer use of advanced construction materials such as fiber-reinforced polymer (FRP) composites. In this case, a fuse can transfer the sudden and dangerous failure mode associated with brittle FRP debonding or rupture to a safe and ductile failure mode at the fuse location. This paper introduces a new type of fused structure as well as an associated design philosophy and approach, in addition to examples of engineering applications.

KEYWORDS fused structures, structural fuse, fiber-reinforced polymer, concrete

1 Introduction

Safety is an important consideration in structural design. A higher safety margin usually requires a heavier structure and consequently higher construction costs. Therefore, safety margin and construction costs are two conflicting goals in structural design. In contrast, safety and costs are generally not considered as conflicting factors in electrical or electronic circuit design. In this application, the important electrical components are protected from damage through the use of a fuse which is embedded within an electrical circuit [1]. The triggering of the fuse stops 'over-loading'. Consequently, measures allowing for over-loading and its associated additional costs are not required. Therefore, the provision of a fuse in electrical circuits eliminates the conflicting nature between safety and cost in the production of electrical devices. In fact, the use of a fuse in an electrical circuit greatly reduces the consequences of failure. In other words, it changes the circuit to possess a safer and less costly failure mode, thereby, providing a cheaper solution. This leads one to ponder the application of the fuse concept to structures. In this case, the incorporation of a fuse should lead to a safer and more predictable failure mode, in addition to a lighter structure.

In structural engineering design, the safety of a structure is taken into account by providing a safety margin through the use of a safety factor (or failure probability in reliability based approaches) [2]. The global safety margin is affected by the reserves (or reliability) allowed in different aspects of design, such as partial safety factors for loadings and materials, and capacity reduction factors for design models [3]. The combination of all reserves or partial safety factors provides the overall (global) safety factor in structural design [4,5]. The global safety factor, however, depends on the failure modes. A more dangerous failure mode requires a higher safety factor (or lower failure probability). For example, the global safety factor for flexural failure without reinforcement yielding (more dangerous) is 30.4% higher than that with reinforcement yielding (less dangerous) [6]. In other words, a less dangerous failure mode requires a smaller safety factor or lighter structure, which provides a more economical construction. Therefore, the exact function of a fuse is to change a more

Article history: Received Jul 31, 2018; Accepted Aug 21, 2018

dangerous failure mode to a less dangerous one.

Numerous studies on different structural fuses have been reported in the literature and in a majority of cases, dissipation of energy from over-load due to seismic attack has been the motivator [7–10]. Fuses have been incorporated into a variety of structural forms, materials and loading scenarios. In each case, the fuse facilitates composite action among the structural components under normal loads [8]. Then, in the case of over-load, the fuse acts as a sacrificial element thus protecting the various structural components that it is attached to. Several structural applications are provided herein. For the case of the seismic design of structures, passive energy dissipation devices are implemented as structural fuses in order to enhance structural performance by reducing seismically induced structural damage [11,12]. Buckling restraint braces have been used as fuses in RC bridge bents. In this case, the fuses have been incorporated as a seismic retrofit measure post bridge construction [7]. In addition, Kauffman and Memari [8] incorporated fuses into multi-story steel frames that contained masonry infill walls. The fuses, which were made from timber disks that connected the masonry walls to the steel frames, allowed forces to be transferred at low loads. At high loads though the disks allowed the masonry infill to separate from the frame, thus protecting the infill.

This paper presents a new type of structural fuse that has been driven by the need to introduce ductility into concrete structures reinforced with fiber-reinforced polymer (FRP) composites. Details of the fuse are provided followed by a design and costing methodology. The approach presented can, however, be used generically for a variety of structural systems and materials, as well as fuse types.

2 A new type of structural fuse

2.1 Ductility problem

Ductility is important to structures and in reinforced concrete (RC) structures it mainly comes from the yielding of tension reinforcement in current practice. When the tension reinforcement in an RC member does not yield at failure (e.g., over-reinforced beams or columns with high axial load level, and FRP-reinforced members), the member has little ductility.

The non-corrosive reinforcement, FRP, is a potentially ideal replacement to steel reinforcement in reinforced concrete [13]. Apart from its non-corrosive nature, it is also much lighter, stronger, and with higher fatigue resistance. Existing studies have shown that despite the current higher initial material cost of carbon FRP (CFRP) bars, bridges constructed with CFRP can be cost effective compared with steel-reinforced bridges in the long-term [14–17]. For example, Grace et al. [18] has shown the reinforcement of concrete bridges with FRP bars to be the least expensive option after 20 years of service. Despite the superior material properties and long-term cost effectiveness though, FRP has not been commonly used in construction mainly due to two shortcomings of the FRP: higher initial material cost and non-ductile failure mode which largely reduces structural ductility [13,19].

Extensive efforts have been reported in the open literature to resolve the ductility problem of FRP reinforced concrete members. Such studies have involved [19]: 1) designing as over-reinforced members and increasing concrete ductility by providing confinement; 2) making use of progressive rupture of prestressed FRP reinforcement by applying different stresses in different layers of FRP; 3) combining prestressed FRP tendons with conventional steel bars to avoid complete loss of tensile resistance at FRP rupture; 4) using unbonded tendons to utilize the deformation of the whole unbonded length; 5) designing the interface between FRP reinforcement and concrete to trigger debonding failure when the stress in the FRP reaches a threshold level; 6) designing the cross-section of a member to proportionate the reinforcement in order to take advantage of the full strain capacity of concrete simultaneously with that of the reinforcement. These methods can achieve certain levels of effectiveness. However, they are less than ideal for several reasons such as too complicated, significantly increasing design and construction costs, or providing limited increases in ductility [19].

For FRP reinforced concrete structures, the only solution recommended by ACI 440.1R-15 [20] to the ductility problem is to design for a higher strength reserve or to over-design the member. Nevertheless, similar to the elastic design philosophy in earthquake engineering, over-design is not only uneconomical but often impractical or impossible in many cases especially for large structures such as large-span bridges. Therefore, conventional structural technologies cannot provide a solution to this ductility problem. Leading authorities have long pointed out that 'unless ductility requirements are satisfied, FRP materials cannot be used reliably in structural engineering applications' [19]. This critical problem has been neglected by the research community thus far. As a result, there is little progress in the practical use of FRP bars to replace steel bars in construction. This is ironic considering that originally the main targeted area of FRP application in construction was for the replacement of steel reinforcement [13].

2.2 An unconventional solution to the ductility problem

Large flexural deformations that occur in structural members are mainly concentrated in a small area of limited length that is referred to as the plastic hinge zone [21]. For conventional RC structures (e.g., over-reinforced RC beams), ductility is obtained from the yielding of reinforcement in the tensile side of the plastic hinge zone as shown in Fig. 1(a). When plastic rotation in the plastic hinge cannot be achieved through plastic elongation or yielding of the reinforcement on the tension side, the other way to achieve it is by shortening or compression yielding on the opposite compression side as shown in Fig. 1(b). This observation triggered a very simple idea: replacing the concrete in the compression zone of the plastic hinge with a strong but more ductile material so that both strength and ductility can be achieved. This idea addresses the ductility problem from a fundamentally different point of view.

The biggest challenge in realizing compression yielding (CY) was to find a suitable CY material. Material scientists have claimed that such a material does not exist. After extensive research works, an ideal material for CY, slurry infiltrated fiber concrete (SIFCON) with perforation (Fig. 2(a)), was made [22]. SIFCON is an existing material that is much more ductile than other cement materials [23], as shown in Fig. 3. However, it still cannot satisfy the excessive ductility demand of a CY system [24]. By providing perforation (holes) inside a SIFCON block, the material becomes an ideal CY material as shown by the SIFCON P-block in Fig. 3. More details of the CY material can be found in Ref. [22]. Experimental, numerical, and analytical studies on CY beams and columns demonstrated that this new method is not only feasible but also highly effective (Fig. 2(b)) that can lead to potentially unlimited ductility [22,24–28].

2.3 New structural fuse

The CY block is an extraordinarily ductile concrete material [22] that is designed to yield before the tension reinforcement reaches its fracture stress. Apart from providing ductility, the CY block can also act as a fuse in the structural system. When accidental excessive loading occurs, the fuse can be designed to activate and force the structural system to deform excessively but in a ductile manner in the fuse location, as shown in Fig. 2(b). When excessive deflection is observed, further overloading can be stopped and subsequent dangerous failure modes such as abrupt FRP rupture, concrete crushing, or shear failure can be avoided.

The use of the fuse (i.e., CY block) produces the following effects:

1) It inhibits further increase of loading by triggering the ‘fuse’. As there is no chance to further increase load, the partial safety factor for loading can be reduced.

2) It transforms a more dangerous failure mode to a safer one, thus reducing the amount of damage at failure. Repair of the member is therefore confined to localized replacement of the fuse (i.e., precast CY block) rather than the whole beam. As a result, a smaller safety margin (or higher failure probability) can be applied which leads to more economical construction.

3 Design philosophy of the fused structures

Due to the change of failure consequences, the requirements and considerations on the structural design are different. The design framework is different from conventional structural design from consideration of loading, evaluation of reliability index or partial safety factors, and the structural design approach.

3.1 Determination of reliability index

As mentioned previously in this paper, the safety margin of structures containing a fuse can be lower than structures that do not contain a fuse. This is on account of fused

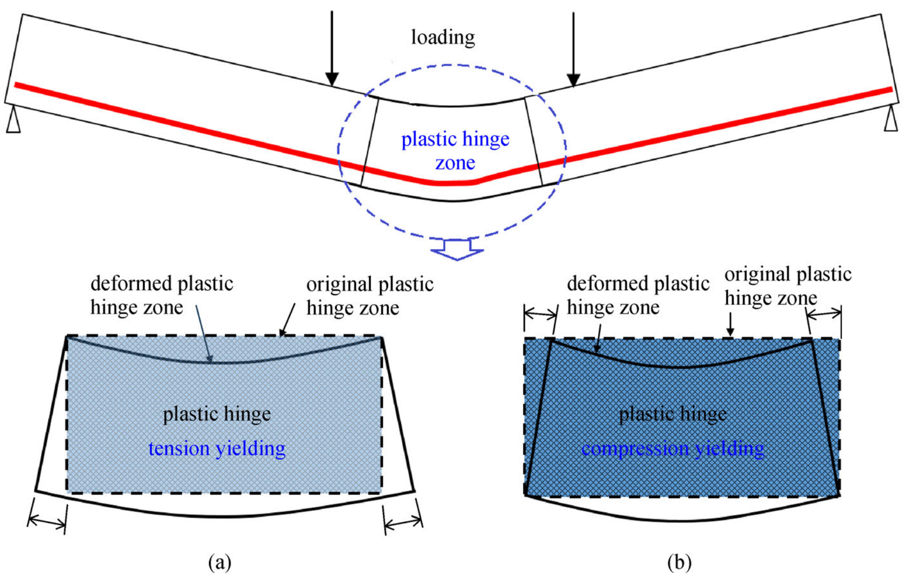

Fig. 1 Plastic deformation in plastic hinge zone. (a) Conventional RC member; (b) CY member.

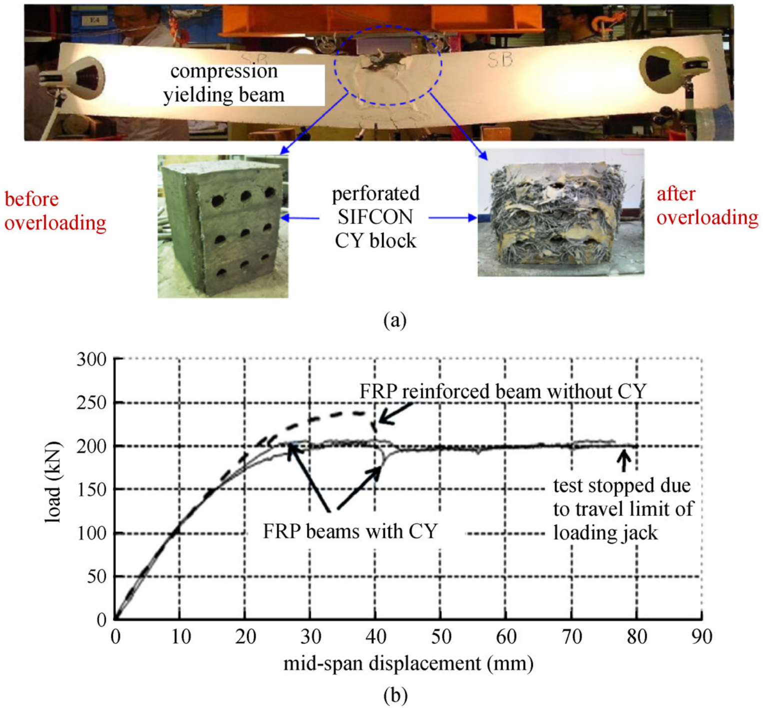

Fig. 2 Compression yielding structural system. (a) CY block cast into an RC beam; (b) test results of CY beams.

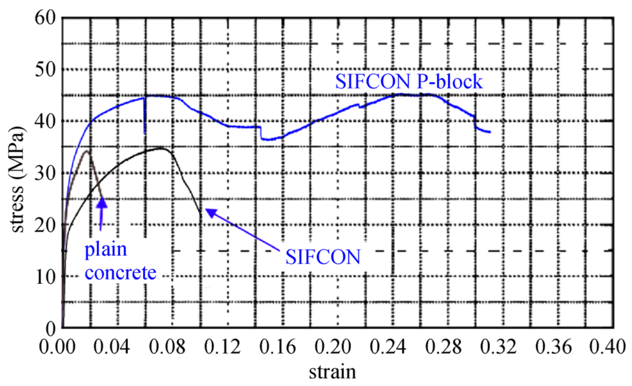

Fig. 3 Stress-strain curves of non-ductile and ductile materials.

structures possessing a safer ductile failure mode. As a result, the consequences of failure are less severe as only fuse replacement costs as well as service interruption costs need to be considered. Therefore, the safety factors or failure probability used for the design of RC structures containing a fuse should be different from those of conventional RC structures that do not contain a fuse. A reliability-based approach can therefore be adopted to calculate a suitable safety factor or failure probability of the new structure.

Neglecting maintenance, demolition, and associated indirect costs (e.g., losses due to service interruption), the total cost C_t can be viewed as the product of failure probability P_f and failure cost C_f plus the initial cost [29]. This can be described as follows

$$C_t = C_i + P_f C_f, \tag{1}$$

where C_i and C_f are initial and failure costs, respectively. It is noted that the initial cost C_i increases with an increase of reliability index β, because a safer structure normally requires higher initial costs. Generally, P_f is a decreasing function of β since the failure probability decreases with increasing reliability index β. In addition, C_f is believed to be independent of β or P_f.

According to Nowak and Collins [29], the relationships between C_i and β as well as P_f and β can be approximately expressed as

$$C_i = a(1 + b\beta), \tag{2}$$

$$P_f = c\exp(-\beta/d), \tag{3}$$

in which a, b, c, and d are constants. Thus, Eq. (1) becomes

$$C_t = a(1 + b\beta) + c\exp(-\beta/d)C_f. \tag{4}$$

Equation (4) consists of two parts that are both functions of β. The first part is an increasing function of β, whereas the second part is a decreasing one. The qualitative relationship between C_t and β is shown in Fig. 4. It is evident that an optimum design can be achieved by adopting a certain value of β that minimizes the total cost C_t. This optimal value of β is the target reliability index β_T, as shown in Fig. 4.

As the use of the fuse does not cause a significant increase in construction costs, the first part of Eq. (4) is considered the same for both conventional and new

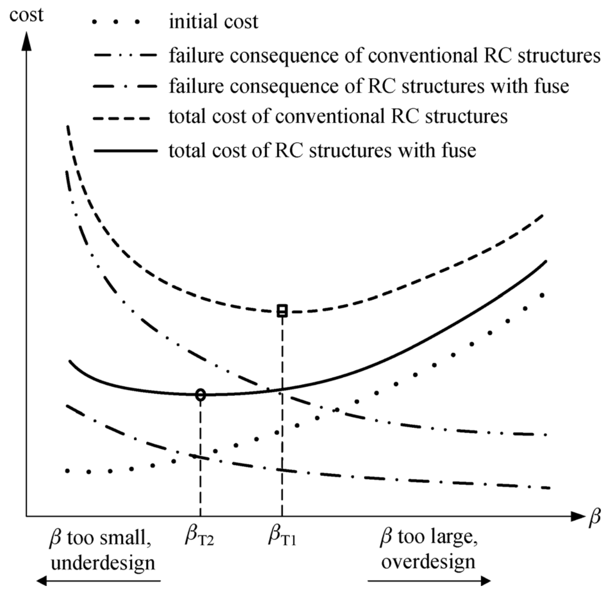

Fig. 4 Costs versus reliability index.

structures, that is, the initial cost in Fig. 4. The failure of the new structure is simply the replacement of the fuse. Therefore, the cost of failure, or the second part of Eq. (4), C_t, is much smaller for new structures (Fig. 4). It can also be seen in Fig. 4 that at the target reliability index, both the failure cost and the total cost C_t are smaller for new structures with a fuse compared with conventional structures that do not contain a fuse. In the meantime, the new structure will have a lower cost if the same reliability index as used in conventional structures is adopted. This is shown in Fig. 4 and the analysis demonstrates the economic advantage of the new structure.

Normally, the target reliability index β_T for a structural component is provided by codes and such index values may differ between codes. In China, the target reliability index β_T at the ultimate limit state under a 50-year reference period is determined by considering both the safety measures and failure modes [30], as summarized in Table 1. Since the use of a fuse in RC structures can prevent dangerous failure modes and minimize losses by avoiding structure collapse, RC structures containing a fuse can have a smaller design reliability index β.

3.2 Design of a fused beam

As shown in Fig. 5, the fused beams involve additional variables in relation to the CY fuse such as material properties and CY zone dimensions. This in turn introduces additional complexity in member design. Considering that the CY block has a higher shear resistance due to the existence of fibers and a roughened surface at the interface with the concrete beam (Fig. 5), the shear strength in the plastic hinge zone and at the interface is higher than that of normal RC beams. Therefore, shear design of CY beams can be based on that for conventional RC beams as a conservative approach.

Compared with conventional RC beams, the flexural behavior of fused beams has another three variables or parameters (Fig. 5), namely 1) height and width ratios of the CY block η and α, 2) the reinforcement ratio ρ_f, and 3) four variables related to the material properties of the CY block (Fig. 6) that include the relative yield strength f_b/f_c (where f_b and f_c are the yielding strength of the CY block and concrete strength, respectively), the yield strain ε_{by}, the ultimate strain ε_{bu}, and the strain hardening/softening modulus ratio ξ.

Table 1 Target reliability index β_T at ultimate state of structures under 50-year period

structural class	consequences of failure	target reliability index β_T	
		ductile failure	brittle failure
class I	high	3.7	4.2
class II	medium	3.2	3.7
class III	low	2.7	3.2

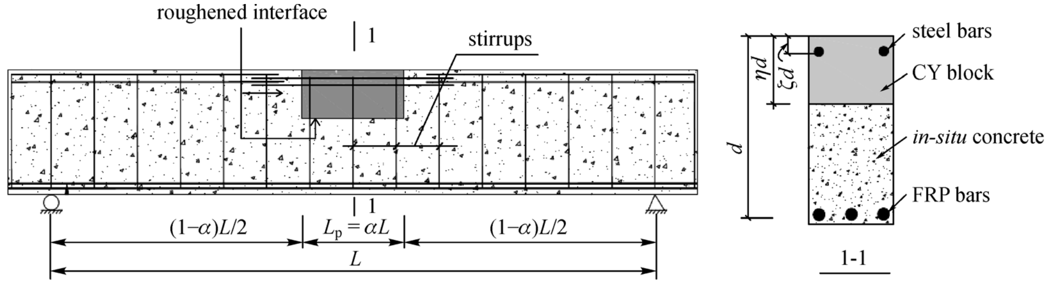

Fig. 5 Structural configuration of an RC beam containing a fuse.

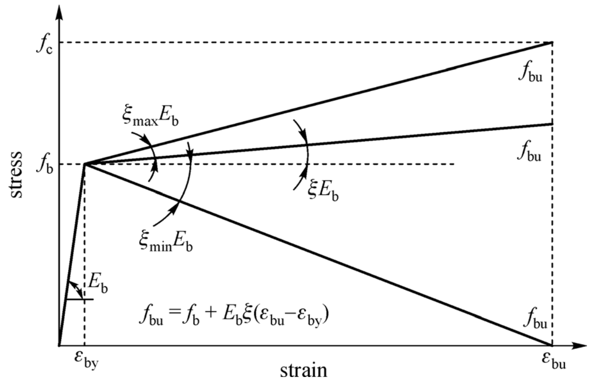

Fig. 6 Stress-strain model of CY block.

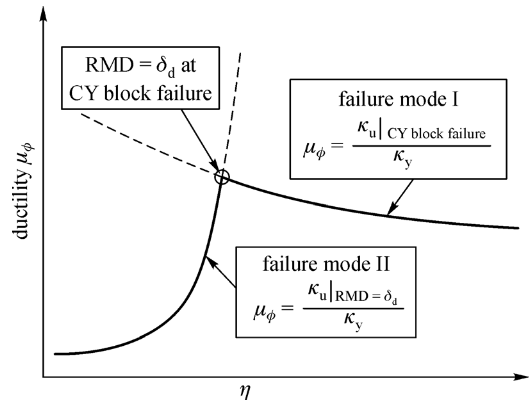

Fig. 7 Optimal curvature relationship.

A performance-based design methodology that explicitly and quantitatively addresses the ductility and strength requirements of fused beams has been developed [22]. As a certain requirement can be fulfilled by different designs with different dimensions and material properties of the CY block, the method provides an optimal design approach that delivers the maximum possible ductility with a minimum CY block. To facilitate convenient use by engineers, the optimal design approach is criterion-based in order to avoid the use of numerical optimization.

As the displacement ductility is directly related to curvature ductility [22], the optimal solution can be found by two steps. First, the optimal curvature ductility is found (i.e., determine a set of values for ξ, f_b, and η at which the optimal curvature is achieved). Secondly, the plastic hinge length ratio, α, from Eq. (5) [22] is determined.

$$\mu_\Delta = \frac{\alpha(2-\alpha)\mu_\varphi + 8\lambda(1-\alpha)^2\dfrac{(EI)_p}{(EI)_e}}{\alpha(2-\alpha) + 8\lambda(1-\alpha)^2\dfrac{(EI)_p}{(EI)_e}}, \tag{5}$$

where μ_Δ and μ_φ are respectively the displacement ductility and curvature ductility ratios; $(EI)_e$ is the rigidity of the fused beam outside the CY zone; $(EI)_p$ is the elastic flexural rigidity of the CY section before yielding; and λ is a factor that depends on the load distribution. For a uniformly distributed load, λ = 5/48 [22].

There are two possible failure modes for fused beams: 1) failure mode I- CY block failure, which is governed by the attainment of the ultimate strain ε_{bu} in any part of the CY block; and 2) failure mode II- the moment resistance after reaching the peak drops below the allowable limit δ_d before CY block failure (i.e., the rate of the moment drop (RMD)$\geqslant \delta_d$ at CY block failure). Wu et al. [22] obtained the relationship between the curvature ductility and the height ratio of the CY block η as shown in Fig. 7. It is clearly visible in Fig. 7 that the intersection point of the two curves for failure modes I and II is an optimal curvature. In other words, the optimal ductility of the CY section is achieved when the failure of the CY block at $\varepsilon = \varepsilon_{bu}$ occurs simultaneously with the onset of the maximum allowable rate of moment drop at RMD = δ_d. In mathematical form, the optimal ductility is achieved when

$$\frac{M_m - M_{min}}{M_m} = \delta_d, \tag{6}$$

where M_{min} is the failure moment which can be determined according to key features of the moment-curvature curve [22]; and M_m is the peak moment of the fused beam. The determination of M_{min} can be found in the work by Wu et al. [22].

In addition to the ductility requirement, the CY beam has to meet the following strength requirement

$$M_m \geqslant M_d, \tag{7}$$

where M_d is the design moment. Therefore, when the strain hardening/softening modulus ratio ξ is considered as a CY material property and treated as a constant in a particular optimal design process, the two remaining variables, f_b and η, can be resolved from Eqs. (6) and (7). In Fig. 7, κ_y and κ_u respectively refer to curvature at yield and ultimate. The optimal curvature, μ_f, can be subsequently substituted into Eq. (5) to calculate the length of the CY block α when the target displacement ductility μ_Δ is given.

As the CY block behaves elastically at service loading, the design approach at the serviceability limit state can be similar to conventional beams.

4 Application

This section illustrates the advantages of a fused structure by means of an example. Considering a footbridge with two fuses as depicted in Fig. 8, the main structural components of the footbridge consist of two arches, two longitudinal beams, several trusses, and a bridge deck. Since the arches are the key structural elements, the cost of the arches is studied. As the bridge is symmetric, only one arch is used to study cost with and without a fuse by using a reliability-based approach. For simplicity, only dead and live loads are considered.

The equation for the appropriate arch axis of the footbridge is determined so that the arch is only under compression along its axis. This gives the following relationship

$$y = \frac{4f(lx-x^2)}{l^2}, \tag{8}$$

where x and y are the coordinates shown in Fig. 9; l and f are the span and the rise of the arch (Fig. 8), respectively. Both the nominal dead load q_D and nominal live load q_L applied to the arch are assumed to be uniformly distributed. According to GB50068 [30], $q_L = 5$ kN/m^2. In addition, the total weight of the footbridge is estimated to be 9000 kg, thus $q_D = 1$ kN/m^2. From equilibrium, one has

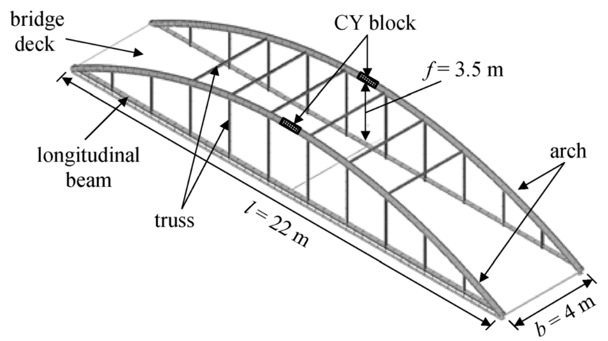

Fig. 8 Schematic diagram of a footbridge containing a CY block fuse in each arch segment.

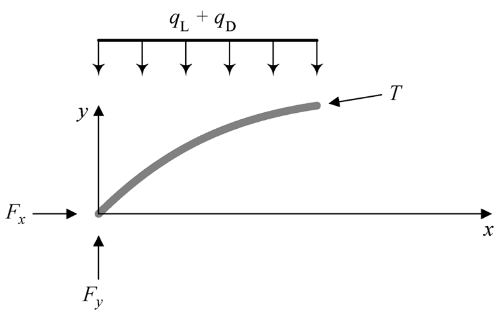

Fig. 9 Free body diagram of the arch.

$$T(x) = \frac{F_x}{\cos\left(\arctan\left(\frac{\mathrm{d}y}{\mathrm{d}x}\right)\right)}, \tag{9}$$

$$F_x = \frac{q_L b l^2}{16f} + \frac{q_D b l^2}{16f}, \tag{10}$$

where $T(x)$ is the compression force along arch axis; F_x is the horizontal force; b is the width of the bridge, respectively (Fig. 8).

The common approach to reliability-based design is the load and resistance factor design (LFRD). Based on ACI318-14 [31] and given that the live and dead loads dominate the design, the LFRD expression under the ultimate limit state can be expressed as:

$$\phi R_n = 1.2D_n + 1.6L_n, \tag{11}$$

where ϕ is the resistance reduction factor; R_n is the nominal resistance; D_n and L_n are the compression force effect given by Eq. (9) due to the nominal dead and live loads, respectively. The coefficients 1.2 and 1.6 are the corresponding partial safety factors for dead and live loads, respectively. The nominal values for D_n and L_n can be obtained from Eq. (9), which are

$$D_n = \frac{\frac{q_D b l^2}{16f}}{\cos\left(\arctan\left(\frac{\mathrm{d}y}{\mathrm{d}x}\right)\right)}, \tag{12}$$

$$L_n = \frac{\frac{q_L b l^2}{16f}}{\cos\left(\arctan\left(\frac{\mathrm{d}y}{\mathrm{d}x}\right)\right)}. \tag{13}$$

The limit state function of this case can be represented by the following equation:

$$Z = R-D-L, \tag{14}$$

in which R, D, and L are random variables for resistance, dead load effect and live load effect, respectively. In reliability analysis, failure occurs if $Z < 0$. That is, the combined load effect ($D + L$) is larger than the resistance (R). Therefore, the failure probability P_f can be expressed as [32]

$$P_f = \Pr(R-D-L<0) = \iiint_{R-D-L<0} f_R(R) f_D(D) f_L(L)\,\mathrm{d}R\mathrm{d}D\mathrm{d}L = 1-\Phi(\beta), \tag{15}$$

where $f_R(R)$, $f_D(D)$, and $f_L(L)$ are the probability density functions for R, D, and L; Φ is the cumulative distribution function of standard normal distribution; and β is the reliability index.

The resistance (R) is assumed to follow a lognormal distribution, in which the mean value equals the nominal value $R_n = (1.2D_n + 1.6L_n)/\phi$ based on Eq. (11). In addition, the coefficient of variation (COV) equals 0.1 [30]. The dead load effect (D) follows a normal distribution with the mean value equal to 1.05 times the nominal value D_n in Eq. (12) while the COV is equal to 0.1 [33]. The live load effect (L) follows an extreme value distribution (type I) with the mean value being equal to the nominal value L_n

in Eq. (13) with a COV of 0.25 [33].

Based on the stochastic information mentioned above, the probability density functions $f_R(R)$, $f_D(D)$, and $f_L(L)$ can be expressed. In the following reliability analysis, resistance factors ϕ ranging from 0.7 to 1.0 with a step size of 0.025 are considered. Since the nominal values for D_n and L_n are known, for a given value of ϕ, the nominal value R_n is given by Eq. (11). Therefore, the reliability index in Eq. (15) can be evaluated by either a Monte Carlo Simulation (MCS) or First Order Reliability Method (FORM) [34] with the detailed probability density functions $f_R(R)$, $f_D(D)$, and $f_L(L)$. The relationship between the resistance reduction factor ϕ and reliability index β can be obtained by repeating this process for each ϕ, as shown in Fig. 10.

According to Table 1, the target reliability index β_T can be 3.7 for a fused structure and 4.2 for a conventional structure. Their corresponding resistance reduction factors ϕ can be obtained based on linear regression, which yields 0.87 and 0.8, respectively, as illustrated in Fig. 10. That means the resistance reduction factor for a structure containing a fuse is larger than a conventional structure, which indicates that the initial cost of materials can be reduced. In addition, for the arch with the fuse, the failure cost is simply the replacement of the fuse and hence significantly lower than that of the arch without a fuse.

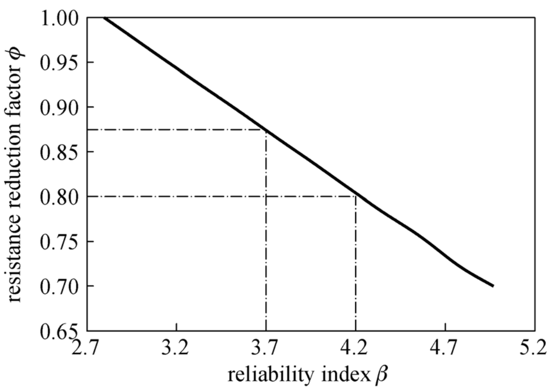

Fig. 10 Relationship between β and ϕ.

5 Conclusions

The concept of incorporating a fuse made of a CY block into a concrete structure has been introduced. It is shown that the addition of a fuse can change the failure mode of the structure and thus reduce the consequences of structural failure. This leads to reduced construction costs. Although this work is based on structures containing a CY block as a fuse, the design philosophy is generic and applicable to many different kinds of structures containing fuses made of a different materials. A reliability-based approach has been presented that demonstrates the economic benefits of fused structures. Due to the change of failure mode, the consequence of failure is changed significantly. As a result, the design reliability index of fused structures should be quite different from those recommended by current design codes which are based on the failure consequences of conventional structures. Future work requires the development of reliability-based design approaches for fused structures that are dependent on the type of fuse used.

References

1. Schossig W. Introduction to the history of selective protection. PAC Magazine, 2007, 70–74
2. Melchers R E. Structural reliability theory in the context of structural safety. Civil Engineering and Environmental Systems, 2007, 24(1): 55–69
3. Stewart M G, Foster S, Ahammed M, Sirivivatnanon V. Calibration of australian standard AS3600 concrete structures part II: Reliability indices and changes to capacity reduction factors. Australian Journal of Structural Engineering, 2016, 17(4): 254–266
4. AS/NZS 1170.0 2002. Structural Design Actions-Part 0: General Principles. Standards Australia, Sydney NSW, 2002
5. Melchers R E, Beck A T. Structural Reliability Analysis and Prediction. West Sussex: John Wiley & Sons, 2017
6. Mosley B, Bungey J, Hulse R, Mosley W H. Reinforced Concrete Design to Eurocode 2. 7th Ed. New York: Palgrave MacMillan, 2012
7. El-Bahey S, Bruneau M. Buckling restrained braces as structural fuses for the seismic retrofit of reinforced concrete bridge bents. Engineering Structures, 2011, 33(3): 1052–1061
8. Kauffman A, Memari A M. Performance evaluation of different masonry infill walls with structural fuse elements based on in-plane cyclic load testing. Buildings, 2014, 4(4): 605–634
9. Li G, Jiang Y, Zhang S Z, Zeng Y, Li Q. Seismic design or retrofit of buildings with metallic structural fuses by the damage-reduction spectrum. Earthquake Engineering and Engineering Vibration, 2015, 14(1): 85–96
10. Shoeibi S, Kafi M A, Gholhaki M. New performance-based seismic design method for structures with structural fuse system. Engineering Structures, 2017, 132: 745–760
11. Cui S. Integrated design methodology for isolated floor systems in single-degree-of-freedom structural fuse systems. Thesis for the Doctoral Degree. Buffalo: State University of New York at Buffalo, 2012
12. Vargas R, Bruneau M. Experimental response of buildings designed with metallic structural fuses. II. Journal of Structural Engineering, 2009, 135(4): 394–403
13. Burgoyne C, Balafas I. Why is FRP not a financial success? In: Proceedings of the 8th International Conerence on FRP Reinforcement for Reinforced Concrete Structures, FRPRCS-8. Patras: University of Patras, 2007
14. Val D V, Stewart M G. Life-cycle cost analysis of reinforced concrete structures in marine environments. Structural Safety, 2003,

25(4): 343–362
15. Eamon C D, Jensen E A, Grace N F, Shi X. Life-cycle cost analysis of alternative reinforcement materials for bridge superstructures considering cost and maintenance uncertainties. Journal of Materials in Civil Engineering, 2012, 24(4): 373–380
16. Ilg P, Hoehne C, Guenther E. High-performance materials in infrastructure: A review of applied life cycle costing and its drivers-the case of fiber-reinforced composites. Journal of Cleaner Production, 2016, 112: 926–945
17. Meiarashi S, Nishizaki I, Kishima T. Life-cycle cost of all-composite suspension bridge. Journal of Composites for Construction, 2002, 6(4): 206–214
18. Grace N F, Jensen E A, Eamon C D, Shi X. Life-cycle cost analysis of carbon fiber-reinforced polymer reinforced concrete bridges. ACI Structural Journal, 2012, 109(5): 697–704
19. Naaman A. FRP reinforcements in structural concrete: Assessment, progress and prospects. In: Fiber-Reinforced Polymer Reinforcement for Concrete Structures, FRPRCS-6. Singapore: World Scientific, 2003, 3–24
20. ACI 440.1R–15. Guide for the Design and Construction of Structural Concrete Reinforced with Fber-Reinforced Polymer (FRP) Bars. Farmington Hills, MI: American Concrete Institute, 2015
21. Paulay T, Priestley M J N. Seismic Design of Reinforced Concrete and Masonry Buildings. New York: John Wiley and Sons, 1992
22. Wu Y F, Jiang J F, Liu K. Perforated SIFCON blocks—An extraordinarily ductile material ideal for use in compression yielding structural systems. Construction & Building Materials, 2010, 24(12): 2454–2465
23. Homrich J R, Naaman A E. Stress-strain properties of SIFCON in compression. In: Fiber Reinforced Concrete Properties and Applications, ACI SP-105. Detroit: American Concrete Institute, 1987, 283–304
24. Wu Y F. Ductility demand of compression yielding fiber-reinforced polymer-reinforced concrete beams. ACI Structural Journal, 2008, 105(1): 104–110
25. Zhou Y W, Wu Y F, Teng J G, Leung A Y T. Parametric space for the optimal design of compression-yielding FRP-reinforced concrete beams. Materials and Structures, 2010, 43(1–2): 81–97
26. Zhou Y W, Wu Y F, Teng J G, Leung A Y T. Ductility analysis of compression-yielding FRP-reinforced composite beams. Cement and Concrete Composites, 2009, 31(9): 682–691
27. Wu Y F, Zhou Y W, He X Q. Performance-based optimal design of compression-yielding FRP-reinforced concrete beams. Composite Structures, 2010, 93(1): 113–123
28. Wu Y F, Zhou Y W. Controlling the damage of concrete columns through compression yielding. Structural Control and Health Monitoring, 2011, 18(8): 890–907
29. Nowak A S, Collins K R. Reliability of Structures. McGraw-Hill, 2000
30. GB50068. Unified Standard for Reliability Design of Building Structures. Beijing: China Building Industry Press, 2001 (in Chinese)
31. ACI 318-14. Building Code Requirements for Structural Concrete and Commentary. Farmington Hills, MI: American Concrete Institute, 2014
32. Rubinstein R Y, Kroese D P. Simulation and the Monte Carlo Method. John Wiley & Sons, 2016
33. Galambos T V, Ellingwood B, MacGregor J G, Cornell C A. Probability based load criteria: Assessment of current design practice. Journal of the Structural Division, 1982, 108: 959–977
34. Huang X, Chen J, Zhu H. Assessing small failure probabilities by AK-SS: An active learning method combining Kriging and subset simulation. Structural Safety, 2016, 59: 86–95